



Numerical Analysis of a Stented Coronary Artery: Investigating Function of Two Stents with Magnesium and Stainless Steel Materials

Y. Taghizadeh, B. Vahidi* , B. Akbari, S. Jalalian Sedaghati

Department of Biomedical Engineering, Faculty of New Sciences and Technologies, University of Tehran, Tehran, Iran.

ABSTRACT: Recently, the use of coronary stents in interventional procedures has rapidly increased. Biodegradable magnesium alloy stents gained increasing interest in the past years due to their potential prospects. However, for the magnesium alloy stents to be feasible for widespread clinical use, it is important that their performance can be compared to modern permanent stents. In this research, a finite element method is used for investigating the effect of the stent geometry and material properties on its behavior. The stent designs made with two different materials, stainless steel 304 and magnesium alloy AZ 31, and the Palmaz-Schatz geometry are modeled and their behavior during the deployment is compared in terms of stress distribution in the stent, vessel wall, plaque as well as in terms of outer diameter changes, radial recoil ratio, axial recoil ratio, and Foreshortening. Moreover, the effect of stent material properties on the restenosis after coronary stent placement is investigated by comparing the stress distribution in the arteries. According to the findings, the possibility of restenosis after coronary stenting is lower for magnesium alloy stents in comparison with the stainless steel 304 stent.

Review History:

Received: 26 Aug. 2017
Revised: 25 Jun. 2018
Accepted: 17 July 2018
Available Online: 2 Aug. 2018

Keywords:

Atherosclerosis
Stent implantation
Restenosis
Foreshortening
Recoil

1- Introduction

Atherosclerosis, the build-up of lipoproteins and hardening of the arteries, is the leading cause of heart attack. In recent years, the use of arterial stents in the treatment of arteriosclerotic vascular disease has been increased and its various models are presented with different geometries and material. Nowadays, with the advancement of related technologies, many researchers have proposed different numerical models for the insertion of stents into the vessel and improved the quality of this procedure [1-3]. In an early research of the stent expansion, Teo et al. [4] performed a stent simulation in order to open blocked blood flow using finite element analysis. In this research, with the omission of the balloon, artery, plaque and the interactions between them and the stent, a single stent model was used to simulate the stent behavior in the vessel. In this modeling, a stent is placed under the influence of uniform internal pressure and after its expansion, the results have been extracted. Due to the simplifications, this model does not provide precise behavior of the intra-vessel stent. In order to increase the accuracy of modeling, contact between the stent and other involved components was considered by Chua et al. [5]. They proposed a balloon-stent model, in which the stent expands indirectly with balloon expansion. In another study, Chua et al. [6] used the balloon-stent model to investigate the effect of Palmaz-Schatz stent geometry on stenting

output; by changing the Palmaz-Schatz stent pattern, such as changing the length and width of the cells, five different models of this kind of stent have been developed and their behavior has been investigated. Walke et al. [7] used a stent-vessel model to evaluate stent diameter variations based on balloon pressure during loading and evaluated the results by performing the test. But due to the absence of balloons and plaques, as well as vessel simulation with a linear elastic model, the results obtained from this study differ greatly from the actual situation. Another model was presented by Lally et al. [8] is the stent-vessel-plaque. This model was used to compare the performance of the two stents when loading. Despite the disadvantages such as excluding the balloon from the model and the simplified assumption of the linear elastic material in the stent, this model became the basis of the work of the next researchers [9, 10]. The main objective of our study is to compare a variety of functional parameters of two particular stents that are very common in clinical use. According to the literature, there's no other research in this area with this attitude.

2. Mathematical Modeling

The different models provided here include stainless steel and magnesium stents with three different types of hypocellular, hypercellular and calcified plaque, with simple blockage and Palmaz-Schatz stent basic geometry. All models are made in Catia software version V5-6R2016.

*Corresponding author's email: bahman.vahidi@ut.ac.ir



Where ΔE is the total energy change, W is total work associated with all the resistance forces (drag, buoyancy, and capillary) and Q is heat change that for an adiabatic system is zero.

2.1. Stent geometry and material properties

Modern structural coronary stents can be divided into three groups according to the structural view: first, open-cell structures such as multiple-stent stents, second, first-generation closed-cell stents, such as the palms stents, and third, later-generated closed cell structure stents such as inflow stents [11]. The shape of open structure stents can change, especially in the areas where cell growth occurs, but the shape of closed structure stents does not change because of the type of their structures. The length and outer diameter and stent thickness are 10, 3 and 0.05 mm, respectively. In this study, the dimensions of the stents are approximately considered based on the former reports [1, 3, 12] in the model calculations. The two-line elastic-plastic material model is also used for the modeling of stents' materials. Mechanical properties of the stent are shown in Table 1.

Table 1. Mechanical properties of the provided stents [2, 12]

	Stainless Steel (304)	Magnesium Alloy (Az31)
Young Modulus (GPa)	193	44
Yield Stress (MPa)	207	138
Tangent Modulus (MPa)	692	633
Poisson Ratio	0.35	0.27

2.2. The Blocked vessel and the plaque model

The artery is assumed to be an ideal, homogeneous, isotropic vessel with the localized block (Fig. 1). For the vessel material, a third-order Mooney-Rivlin hyperelastic non-linear model is used [13].

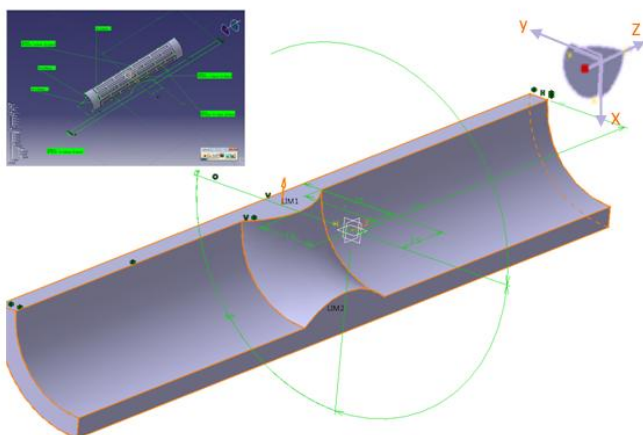


Fig. 1. Computational geometry of the plaque created in the presence of the vessel

Considering the fact that with the progression of atherosclerosis, the plaque composition is altered, in this study, we used the three possible compositions of the plaque. For these three different types of plaques, a third-order Mooney-Rivlin hyperelastic nonlinear model is used as follows (Eq. (1)) [11, 14]:

$$w = C_{10}(I_1 - 3) + C_{01}(I_2 - 3) + C_{20}(I_1 - 3)^2 + C_{11}(I_1 - 3)(I_2 - 3) + C_{30}(I_1 - 3)^3 \quad (1)$$

The percentage of blockage in this study is 25% and it is considered symmetric. The coefficients related to each material are shown in Table 2.

Table 2. The strain energy density function coefficients used for the plaques and the vessel [13, 14]

	C_{01}	C_{10}	C_{11}	C_{20}	C_{30}
Calcified	-495.96	-506.61	1193.53	3637.8	4737.25
Hypocellular	165.111	16.966	955.388	0	0
Hypercellular	-802.723	831.636	1157.68	0	0
Vessel	2.75	18.9	59.043	85.72	0

2.3. The balloon model

The balloon used to expand the stent is made of polyurethane rubber with a length of 12 mm, an outer diameter of 2.9 mm and a thickness of 0.1 mm. The balloon is placed inside the stent and by applying the pressure on its inner surface, is inflated by a special gas, expanding the stent by connecting the two outer surfaces of the balloon and interior of the stent. The polyurethane material has been modeled using a first-order non-linear hyperelastic Mooney-Rivlin model [6, 15].

2.4. Numerical mesh and boundary conditions

In order to reduce the computational costs, symmetric geometry has been used in the model so that instead of modeling the entire stent, balloon, vessel, and plaque, only a quarter of them is considered in the Palmaz-Schatz Stent model. After applying symmetry, appropriate boundary constraints are applied to the points located on the symmetry surfaces. These constraints are the fixed nodes on the cut surfaces in the direction of their vertical vector. For all of the models including the stent and the vessel and the plaque, the balloon is also perfectly symmetrical around its axis and it is completely bounded on both ends. In this study, all the models are simulated using the finite element method in ABAQUS software. For the artery model meshing, a three-dimensional cube element is used. For the stent model, an 8-node linear block element with a reduced-integral approach (C3D8 R) is used. Also, for the vessel and balloon modeling, the linear block of the hybrid (C3D8H) element is used.

2.5. Loading and Numerical Solution

The implicit method is used to solve the problem. The friction coefficient between balloons and stents for all of the models is considered to be 0.055. Loading is applied in four stages: in the first stage, regardless of the presence of the balloons and the stents, the vessel and plaque are affected by an internal uniform pressure of 13.3 kPa, which is equivalent to a mean blood pressure of 100 mm Hg, which expands the vessel and causes tension in its thickness. Applying this pressure makes the model physiologically more relevant. In the next stage, maintaining the initial pressure applied to the vessel and the plaque, in order to expand the stent, a uniformly linear pressure at the rate of 1.635/sec is applied linearly

over the interior surface of the balloon. It is considered such that it would be possible to make a comparison between the models (The maximum load on the models is chosen so that the final diameter of the stents would be equal and they cause a similar change on the vessel diameter). In the third step, the maximum applied load is maintained for 0.2 seconds, and then in the fourth step, the applied load is linearly removed within one second.

To investigate independence of the numerical solution to the mesh size, the process of reducing the errors were monitored by refining the mech. Neglecting a trivial computational error, the results of the models are obtained and presented in this study by choosing a model with 11264 elements.

3. Results and Discussion

In the 304-calcified base model with a pressure of 0.4 MPa, as shown in Fig. 2, the areas with a maximum stress of 257.5 MPa, are located on the quadrilateral cells of the stent, and the probability of failure in these points are higher than other points of the stent. The maximum amount of von mises stress on the vessel in the 304-calcified base model is 0.287 MPa. The higher the amount of this maximum stress, the greater the stent damage to the artery, resulting in increased restenosis after stenting. There is an excessive stress gradient between the inner surface of the artery and its outer surface. This means that the vessel's sensitive and vulnerable points are on its inner surface and they are the points where the maximum diameter change in the stent occurs.

Comparison among the models suggests that in order to create a definite change in the diameter of the vessel, the 304-steel stents produce more stress on the vessel than the magnesium stents. The results show that the use of AZ 31 magnesium alloy stents compared to the stainless steel stents leads to less magnitude of stress on the vessel. Also, by examining the results, it can be seen that the magnesium stents for all three models with different plaques have a higher radial and longitudinal reversibility as compared to the steel stents due to weak radial strength and low yield stress, and low stiffness of the magnesium stents in comparison with the steel stents; which is their only fundamental weakness.

In the 304-stainless steel models, distribution of stress on the arterial wall is not only dependent on the applied pressure but also strongly dependent on the plaque material.

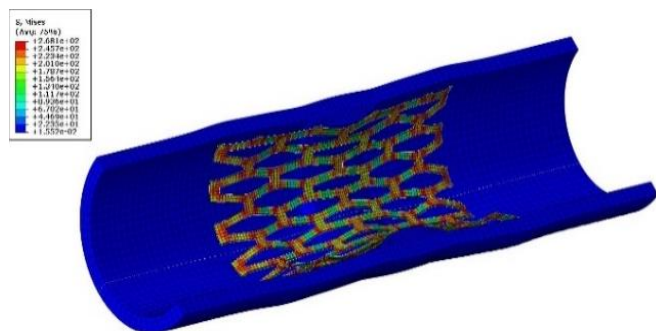


Fig. 2. Distribution of Von Mises stress (MPa) on the stent in the calcified base model -304 with vessel and plaque

The stresses induced on the arterial wall in the calcified and the hypocellular plaques are much lower as compared to the hypercellular plaques. Also, the calcified plaque, in comparison with the hypocellular plaque, causes less stress on the artery wall due to its higher stiffness. The maximum stress produced in the AZ31 calcified plaque is much lower as compared to the 304-calcified base model. Also, for hypocellular and hypercellular plaques in AZ31 models, the maximum tensile stresses have shown to be lower than the 304-calcified base model.

4. Conclusion

In this research, the effects of stent material properties on its function are investigated utilizing the finite element method. This method, in addition to being affordable, doesn't have many limitations which exist in the related clinical studies. The results show that in the simple blockage case, despite the same vessel diameter change in all of the models, the magnitude of the maximum stress produced by the AZ31 magnesium stent is much less than the stainless steel 304 stent. Therefore, it can be predicted that the use of AZ31 stents leads to less damage to the arterial wall cells, resulting in a reduction in the probability of re-closure after stenting. Also, magnesium stents with a thicker geometry, apply much less stress to the arterial wall than the steel stents with the baseline geometry. In overall, in all the cases, the magnesium stents perform better functions than the steel stents. The main problem with magnesium stents as compared with the permanent stents is their low radial strength and their higher reversibility.

References

- [1] S. De Bock et al., "Virtual evaluation of stent graft deployment: A validated modeling and simulation study," *J. Mech. Behav. Biomed. Mater.*, vol. 13, pp. 129–139, Sep. 2012.
- [2] J. A. Grogan, S. B. Leen, and P. E. McHugh, "Comparing coronary stent material performance on a common geometric platform through simulated bench testing," *J. Mech. Behav. Biomed. Mater.*, vol. 12, pp. 129–138, Aug. 2012.
- [3] A. S. Puranik, E. R. Dawson, and N. A. Peppas, "Recent advances in drug eluting stents," *Int. J. Pharm.*, vol. 441, no. 1–2, pp. 665–679, Jan. 2013.
- [4] E. C. Teo, Q. Yuan, and J. H. Yeo, "Design optimization of coronary stent using finite element analysis," *ASAIO J.*, vol. 46, no. 2, p. 201, Mar. 2000.
- [5] S. N. D. Chua, B. J. Mac Donald, and M. S. J. Hashmi, "Finite-element simulation of stent expansion," *J. Mater. Process. Technol.*, vol. 120, no. 1–3, pp. 335–340, Jan. 2002.
- [6] S. N. David Chua, B. J. Mac Donald, and M. S. J. Hashmi, "Finite element simulation of stent and balloon interaction," *J. Mater. Process. Technol.*, vol. 143–144, no. 1, pp. 591–597, Dec. 2003.
- [7] W. Walke, Z. Paszenda, and J. Filipiak, "Experimental and numerical biomechanical analysis of vascular stent,"

- J. Mater. Process. Technol., vol. 164–165, pp. 1263–1268, May 2005.
- [8] C. Lally, F. Dolan, and P. J. Prendergast, “Cardiovascular stent design and vessel stresses: A finite element analysis,” *J. Biomech.*, vol. 38, no. 8, pp. 1574–1581, Aug. 2005.
- [9] C. Capelli, F. Gervaso, L. Petrini, G. Dubini, and F. Migliavacca, “Assessment of tissue prolapse after balloon-expandable stenting: Influence of stent cell geometry,” *Med. Eng. Phys.*, vol. 31, no. 4, pp. 441–447, May 2009.
- [10] W. Wu, W.-Q. Wang, D.-Z. Yang, and M. Qi, “Stent expansion in curved vessel and their interactions: A finite element analysis,” *J. Biomech.*, vol. 40, no. 11, pp. 2580–2585, Jan. 2007.
- [11] A. Kastrati et al., “Influence of stent design on 1-year outcome after coronary stent placement: a randomized comparison of five stent types in 1,147 unselected patients,” *Catheter. Cardiovasc. Interv.*, vol. 50, no. 3, pp. 290–7, Jul. 2000.
- [12] S. N. David Chua, B. J. Mac Donald, and M. S. J. Hashmi, “Finite element simulation of stent and balloon interaction,” *J. Mater. Process. Technol.*, vol. 143–144, pp. 591–597, Dec. 2003.
- [13] C. Lally, F. Dolan, and P. J. Prendergast, “Cardiovascular stent design and vessel stresses: a finite element analysis,” *J. Biomech.*, vol. 38, no. 8, pp. 1574–1581, Aug. 2005.
- [14] I. Pericevic, C. Lally, D. Toner, and D. J. Kelly, “The influence of plaque composition on underlying arterial wall stress during stent expansion: The case for lesion-specific stents,” *Med. Eng. Phys.*, vol. 31, no. 4, pp. 428–433, May 2009.
- [15] F. Ju, Z. Xia, and K. Sasaki, “On the finite element modelling of balloon-expandable stents,” *J. Mech. Behav. Biomed. Mater.*, vol. 1, no. 1, pp. 86–95, Jan. 2008.